BEHAVIOR OF STACKED CRATES DURING EARTHQUAKE

T. Ichinose (I)
M. Murakami (II)
K. Ohami (III)
Y. Hosokawa (IV)
Presenting Author: M. Murakami

SUMMARY

This paper deals with the seismic behavior of stacked crates, which suffered a critical damage during the 1978 Miyagi-ken-oki earthquake. Dynamic properties of the stacked crates were studied through the full scale vibration testings. An analytical method was developed to model the elastic deformation and the rocking motion of the stacked crates into a single degree of freedom system by means of the Galerkin's method. Earthquake response analyses were carried out. It was concluded that the collision between the neighbouring stacked crates columns has played an important role on the collapse of the stacked crates.

INTRODUCTION

During the 1978 Miyagi-ken-oki earthquake in Japan, a lot of stacked crates containing bottles of beer or soft drinks collapsed in warehouses and factories(2), not only causing economic losses but also creating a menace to the safety of workers there.

A lot of experimental and analytical studies have contributed to the rocking motion of the rigid body(2,4), and to the colliding motion of the piled rigid bodies(1,3). However, studies on the dynamic properties of the stacked elastic bodies are few. The damaged crates are made of plastics and easy to deform. Elastic deformation, as well as rocking motion, should be considered to study the seismic response of the stacked crates.

The objective of this study is to clarify the seismic behavior of the stacked crates. Dynamic properties of the stack are studied through the full scale vibration testings. An analytical method is developed to model the elastic deformation and the rocking motion of the stacked crates into a single degree of freedom system by means of Galerkin's method. Earthquake response analyses are carried out.

FULL SCALE VIBRATION TESTS

The stacked crates containing bottles of beer are chosen as the subject of this study. Twenty bottles of beer are ranged in the crate made of plastics. In factories or warehouses, the crates are piled up on a palette to constitute a column in Fig 1, according to whether the bottles are filled or empty. Such columns are crammed side to side as in Fig 2.

(I) Research Associate, Nagoya Institute of Technology, Nagoya, Japan
(II) Professor, Chiba University, Chiba, Japan
(III) Research Associate, Chiba University, Chiba, Japan
(IV) Research Associate, The University of Tokyo, Tokyo, Japan

An assumption is made that every column of stacked crates deforms and rocks in a same phase and in a same period within the crammed columns. Collision and friction between neighbouring columns are ignored. Thus, the vibration tests were carried out upon a single column of stacked crates, using the real bottles, crates, and palettes. Hereafter, the stacks in Fig 1 (a) and (b) are called as 4x4 specimen and 6x3 specimen, respectively.

The stationary vibration tests by a shaking table, the free vibration tests and the forced vibration tests were carried out. The excitation method of the forced vibration test shall be explained later.

The relationships between the observed first mode period T and the top displacement amplitude q of 4x4 specimen are shown in Fig 3, where "short" and "long" indicate the direction of excitation. The chained line shows the theoretical displacement amplitude at the beginning of the rocking motion, which is calculated according to the Appendix. The relations between T and q are approximated by the following linear functions, which are indicated by solid lines in Fig 3.

4x4 short	T=0.029q+1.22	--- (1-a)
4x4 long	T=0.039q+1.02	--- (1-b)
6x3 short	T=0.030q+1.10	--- (1-c)
6x3 long	T=0.040q+1.00	--- (1-d)

From the stationary vibration tests by the shaking table, following observations were obtained, as well.
(a) The damping ratios of the specimens at first mode vibration are approximately 4% or 5%, irrespective of the types of specimens, the directions of excitation, and the displacement amplitude.
(b) Observed first and second vibration modes at small amplitude are similar to those of uniform cantilever beam.
(c) Second mode periods of the specimens are from 0.26 sec to 0.34 sec. The damping factors at second mode are from 6% to 12%.

The collapse mode of the specimen during the forced vibration test is shown in Fig 4. The test was carried out by pulling a rope knotted to the pallete periodically. The lowest layer of the specimen is falling down like the dominos, because the top of every layer is tied with string as in Fig 1.

ANALYTICAL ASSUMPTIONS

In order to reduce the dynamic properties of the stack into the single degree of freedom system, following six assumptions are made.

Assumption (1): Equation of motion of the specimen can be expressed by that of uniform flexural beam as follows.

$$\rho \cdot \frac{\partial^2 u}{\partial t^2} + \gamma \cdot \frac{\partial u}{\partial t} + \frac{\partial^2 M}{\partial y^2} = - \rho \cdot \frac{d^2 u_0}{dt^2} \qquad \text{--- (2)}$$

, where $\rho = W/H$, W and H : total mass and height of the specimen
$U(y,t)$; relative displacement of the specimen from the ground.
γ ; damping coefficient per unit length.
$M(y,t)$; bending moment distribution.
$u_0(t)$; displacement of the ground.

Assumption (2): While the top displacement q is less than the uplifting displacement s_n, the specimen deforms in the first mode of the uniform cantilever beam U(y), as the following equation. Higher modes are ignored, because the overturning moments of the higher modes are much less than that of the first mode.

During $-s_n < q(t) < s_n$,

$$u(y,t) = U(y)\cdot q(t) \quad \text{---- (3)} \qquad s(t) = q(t) \quad \text{--- (4)}$$

$$U(y)=Ls(\cosh \lambda\xi - \cos \lambda\xi)-Lc(\sinh \lambda\xi - \sin \lambda\xi) \quad \text{---------- (5)}$$

$$\xi = y/H \quad , \quad \lambda=1.8751$$

$$Ls=(\sinh \lambda + \sin \lambda)/2(\cosh \lambda \sin \lambda - \sinh \lambda \cos \lambda)$$

$$Lc=(\cosh \lambda + \cos \lambda)/2(\cosh \lambda \sin \lambda - \sinh \lambda \cos \lambda)$$

Assumption (3): While q is greater than s_n, the rocking component r(t) is added to the elastic deformation s(t) as in the following equations. The component of the elastic deformation s(t) results in zero when q reaches at the unstable displacement r_n, which is calculated according to the Appendix.

When $q(t) > s_n$ or $q(t) < -s_n$,

$$u(y,t) = U(y)\cdot s(t) + (y/H)\cdot r(t) \quad \text{--- (6)} \qquad r(t)= \frac{q(t)-s_n}{r_n - s_n} \cdot r_n \quad \text{--- (8)}$$

$$s(t)=\frac{r_n-q(t)}{r_n-s_n} \cdot s_n \quad \text{-------- (7)} \qquad q(t)=s(t) + r(t) \quad \text{--- (9)}$$

Assumption (4): Secant rigidity of flexure K is uniform along the height of the specimen, and depends only upon the component of the elastic deformation s(t). Thus, the moment distribution M(y,t) becomes:

$$M(y,t) = K(s)\cdot\frac{\partial^2 u}{\partial y^2} = K(s)\cdot s(t)\cdot\frac{d^2U}{dy^2} \quad \text{---- (10)}$$

Relationship between K and s is approximated as follow, using eqs(1) and substituting q=s.

$$K(s)=\rho\cdot(H/\lambda)^4\cdot(2\pi/T)^2 \quad \text{---------- (11)}$$

$$T=as+b \qquad a,b : \text{constants in eqs(1)}$$

Assumption (5): The damping coefficient γ is proportional to the tangential stiffness of the specimen, except during the rocking motion.

$$\gamma=c\cdot d(K\cdot s)/ds \quad , \; c=\text{const.} \quad \text{---------- (12)}$$

Damping is ignored ($\gamma=0$) while the rocking motion exists.

Assumption (6): The velocity at the top of the specimen changes at the instance of the uplifting and the landing as shown in Fig 5, due to the conservation of angular momentum around the axis of rotation i and j.

SINGLE DEGREE OF FREEDOM MODEL

(a) Equation of motion before uplifting

Substituting the deformation mode, eq(3), the moment distribution, eq(10), and the damping coefficient, eq(11), into the basic equation of motion eq(2), and noting that

$$d^4U/dy^4=(\lambda/H)^4\, U \quad \text{--- (13)}$$

the following equation is obtained.

$$\rho \cdot U \cdot \ddot{q} + c \cdot \frac{d(K \cdot s)}{ds} \cdot U \cdot \dot{q} + \left(\frac{\lambda}{H}\right)^4 \cdot K \cdot U \cdot q = - \rho \ddot{u}_0 \qquad \text{--- (14)}$$

According to Galerkin's method, both sides of the eq(14) are multiplied by u=U.q, and integrated from y=0 to H, resulting into:

$$\rho \cdot \ddot{q} + c \cdot \frac{d(K \cdot s)}{ds} \cdot \dot{q} + \left(\frac{\lambda}{H}\right)^4 \cdot K \cdot q = - \rho \cdot \beta_1 \cdot \ddot{u}_0 \qquad \text{--------- (15)}$$

where $$\beta_1 = \int_0^H U \cdot dy \Big/ \int_0^H U^2 dy = 1.564 \qquad \text{--------- (16)}$$

Multiplying the both sides of the above equation by $\int U\, dy$, and defining the base shear force F(s) by the following equation,

$$F(s) = \int_0^H \frac{\partial^2 M}{\partial y^2} \cdot dy = K \cdot s \cdot \left(\frac{\lambda}{H}\right)^4 \int_0^H U \cdot dy \qquad \text{---------- (17)}$$

the equation of motion of the reduced SDOF system is obtained.

$$M_e \cdot \ddot{q} + C_e \cdot \frac{dF(s)}{ds} \cdot \dot{q} + F(s) = - M_e \cdot \beta_1 \cdot \ddot{u}_0 \qquad \text{--- (18)}$$

$$M_e = \rho \cdot \int_0^H U \cdot dy \quad \text{--- (19)} \qquad C_e = c \cdot (H/\lambda)^4 \quad \text{--- (20)}$$

The explicit form of F(s) is derived as follows by substituting eq(11) into eq(17).

$$F(s) = \rho \cdot s \cdot (2\pi/T)^2 \cdot \int_0^H U \cdot dy = M_e \cdot s \cdot (2\pi/T)^2 \qquad \text{--- (21)}$$

(b) Equation of motion during uplifting

According to the assumption (5) that $\gamma=0$ during uplifting, the basic equation of motion, eq(2), reduces to:

$$\rho \cdot \frac{\partial^2 u}{\partial t^2} + \frac{\partial^2 M}{\partial y^2} = - \rho \cdot \frac{d^2 u_0}{dt^2} \qquad \text{--- (22)}$$

Substituting the deformation mode during uplifting, eqs (6), (7) and (8), into the above equation, and defining the velocity distribution V(y) as

$$V(y) = - \frac{s_n}{r_n - s_n} \cdot U(y) + \frac{r_n}{r_n - s_n} \cdot \frac{y}{H} \qquad \text{--- (23)}$$

, following equation is obtained.

$$\rho \cdot V \cdot \ddot{q} + \left(\frac{\lambda}{H}\right)^4 \cdot K \cdot U \cdot s = - \rho_0 \cdot \ddot{u}_0 \qquad \text{--- (24)}$$

According to the Galerkin's method, both sides of the eq(24) are multiplied by u(y,t) and integrated from y=0 to H, resulting into :

$$M_e \cdot \ddot{q} + \nu_2 \cdot F(s) = - M_e \cdot \beta_2 \cdot \ddot{u}_0 \qquad \text{-------- (25)}$$

$$\nu_2 = \int_0^H U \cdot u \cdot dy \Big/ \int_0^H V \cdot u \cdot dy \quad \text{--- (26)} \qquad \beta_2 = \int_0^H u \cdot dy \Big/ \int_0^H V \cdot u \cdot dy \quad \text{--- (27)}$$

, where the base shear factor ν_2 and the participation factor β_2 are dependent on the top displacement q.

(c) Unified equation of motion

The reduced SDOF equation of motions, eqs (18) and (25) are combined and expressed as :

$$M_e \cdot \ddot{q} + C_e \cdot \frac{dF(s)}{ds} \cdot \dot{q} + \nu \cdot F(s) = - M_e \cdot \beta \cdot \ddot{u}_0 \qquad \text{--- (28)}$$

,where $|q| < s_n$ ---- C_e=eq(20) , ν=1 , β=eq(16) , s=eq(4)
$|q| > s_n$ ---- C_e=0 , ν=eq(26) , β=eq(27) , s=eq(7)

The relationships between ν , β and q are calculated for the specimens and shown in Fig 6. The values ν and β change at $|q|=s_n$, because the velocity distribution changes from U(y) to V(y).

Relationship between the base shear force F and q is calculated substituting eq(4) or eq(7) into eq(21). F is the one-valued odd function of q, i.e. the reduced system is nonlinear-elastic. An example of F is shown in Fig 7.

If the flexural rigidity K becomes infinitely large, eq(28) converges to the equation of motion of the rigid body.

(d) Conservation of angular momentum

At the instance of uplifting shown in Fig 5(c)(d), the top velocity changes from q to $\zeta_1 q$, according to the assumption (6). The dotted portion and the hatched portion in Fig 5(d) rotates round the points i and j, respectively. The angular momentums of the 4x4 specimen(short) just before and after the uplift, I_{BU} and I_{AU}, are calculated as follow.

$$I_{BU} = \rho \cdot \dot{q} \cdot \left\{ \int_0^H U \cdot y \cdot dy + \frac{B^2}{12} - \frac{B^2}{16} \cdot U\left(\frac{H}{4}\right) \right\} \qquad \text{--- (29)}$$

$$I_{AU} = \rho \cdot \zeta_1 \cdot \dot{q} \left\{ \int_0^H V \cdot y \cdot dy + \frac{B^2}{12} - \frac{B^2}{16} \cdot V\left(\frac{H}{4}\right) + \frac{13}{64} \cdot B^2 \cdot \frac{r_n}{r_n - s_n} \right\} \qquad \text{--- (30)}$$

Equating I_{BU} to I_{AU}, the value ζ_2 is obtained. The values ζ_2 of another specimen or direction can be derived in a similar way.

At the instance of landing shown in Fig 5(a)(b), the top velocity changes from q to q/ζ_2. The angular momentums of the 4x4 specimen (short) just before and the landing, I_{BL} and I_{AL}, are caluculated as follow.

$$I_{BL} = \rho \cdot \dot{q} \left\{ \int_0^H V \cdot y \cdot dy + \frac{B^2}{12} - \frac{B^2}{16} \cdot V\left(\frac{H}{4}\right) - \frac{13}{64} \cdot B^2 \cdot \frac{r_n}{r_n - s_n} \right\} \qquad \text{--- (31)}$$

$$I_{AL} = \rho \cdot \frac{\dot{q}}{\zeta_2} \cdot \left\{ \int_0^H U \cdot y \cdot dy + \frac{B^2}{12} - \frac{B^2}{16} \cdot U\left(\frac{H}{4}\right) \right\} \qquad \text{--- (32)}$$

Equating I_{BL} to I_{AL}, the value ζ_2 is obtained.

EARTHQUAKE RESPONSE ANALYSIS

In this section, base shear force F is simplified as shown in Fig 8, connecting three points at 3/4 of the maximum strength, $q=s_n$, and $q=r_n$. Input data for the earthquake response analysis are shown in Table 1. The effective

damping coefficient C_e in eq(28) is determined so that the damping factor h_e be 5% with respect to the initial stiffness K_0:

$$h_e = \frac{C_e}{2}\cdot\sqrt{\frac{K_0}{M_e}} = 0.05 \quad \text{--- (33)}$$

The participation factor β and the base shear factor ν are also simplified, i.e., β and ν values during the uplifting are averaged from $q=s_n$ to $q=r_n$ as shown in the parentheses in Table 1.

An example of time history response is shown in Fig 9, using the NS component of the Miyagi-ken-oki earthquake in June, 1978. The broken lines in the displacement response indicate the uplifting displacement s_n. The base shear response has several hollows where the top displacement is greater than s_n, because the base shear decreases at $|q| > s_n$. Although the maximum displacement is as large as 3 times of the uplifting displacement, the specimen does not result in collapse.

The response analyses are conducted using the above mensioned earthquake record multiplied by 0.6 to 2.0. The maximum displacement response of the specimens are shown in Fig 10. The maximum response does not necessarily increase as the magnification factor is increased. This tendency is similar to that of the response of the rigid body. It should be noted that the probability of the complete collapse in relatively small even if the stack is exited by a fairly large earthquake. Therefore the damage during the 1978 Miyagi-ken-oki earthquake cannot be entirely attributable to the first mode vibration and rocking motion alone. The collision and friction between the neighbouring columns of the stacked crates should have played an important role.

CONCLUDING REMARKS

Dynamic properties of a column of stacked cretes are modelled and reduced into SDOF system by Galerkin's method, considering the elastic deformation and the rocking motion. It is concluded that the collision and friction between the neighbouring columns of the stacked crates should have played an important role in the actual damage during the earthquake.

ACKNOWLEDGEMENTS

The authors appreciate the great contribution by Prof. H. Aoyama and Prof. S. Otani of the University of Tokyo, for their valuable guidance and suggestions throughout the study.

APPENDIX

The overturning moment M_o is obtained by integrating the inertia force:

$$M_o = \int_o^H \frac{\partial^2 M}{\partial y^2}\, y\cdot dy = K\cdot s\cdot\left(\frac{\lambda}{H}\right)^4 \int_o^H U\cdot y\cdot dy \quad \text{--- (34)}$$

Substituing eq(11) into eq(34), M_o reduces to:

$$M_o = \rho\cdot\left(\frac{2\pi}{as+b}\right)^2 \cdot \int_o^H U\cdot y\cdot dy \quad \text{--- (35)}$$

The resisting moment M_R of 4x4 (short) is expressed as follows.

$$M_R = \frac{7}{16}\cdot\rho\cdot g\cdot H\cdot B - \rho\cdot g\cdot\int_0^H u\cdot dy \qquad \text{--- (36)}$$

where g: gravity acceleration
B: width of the specimen along the direction of excitation.

The coefficient (7/16) differs for different specimen or different direction of excitation. The uplifting displacement s_n is obtained equating M_O to M_R and substituting $s=s_n$ and $u=s_n\cdot U$. The unstable displacement r_n is obtained equating M_R to zero and substituting $u=r_n\cdot(y/H)$.

REFERENCES

(1) Ikushima, T. and Kawakami, M. "Seismic Response Analysis for block-type Fuel HTGR Core", 3rd SMiRT(London) K8/7, Sep. 1975, 10pp.
(2) "Report on the damage by 1978 Miyagi-ken-oki earthquake (in Japanese)", Architectural Institute of Japan, Feb. 1980, 908pp.
(3) Aslam, M., Godden, W.G. and Scalise, D.T. "Earthquake Rocking Response of Rigid Bodies", Journal of the Structural Division, ASCE, Vol 106, No.ST2, Feb. 1980, pp.377-392.
(3) Muto, K. and Kuroda,T., "Experimental and Analytical Studies on Seismic Response Behavior of HTGR Core, Part I - Experimental Study-", Transactions of Architectual Institute of Japan, No.290, Apr. 1980, pp.95-106.
(4) Ishiyama, Y., "Criteria for Overturning of Bodies by Earthquake Excitations", Transactions of Architectual Institute of Japan, No.317, July 1982, pp.33-47.

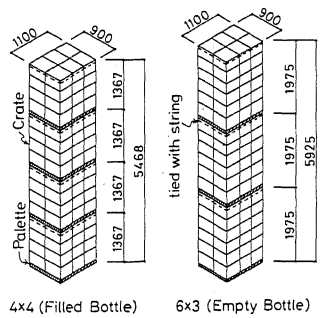

Fig 1 Tested and analyzed column of stacked crates

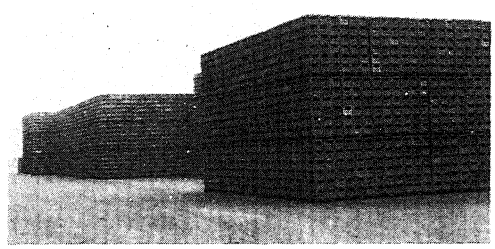

Fig 2 Piled stack of crates (empty bottle)

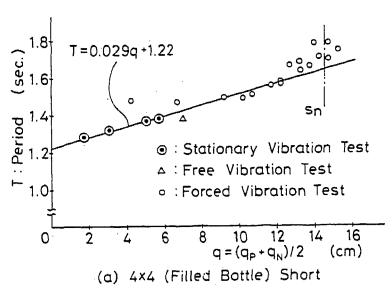

(a) 4x4 (Filled Bottle) Short

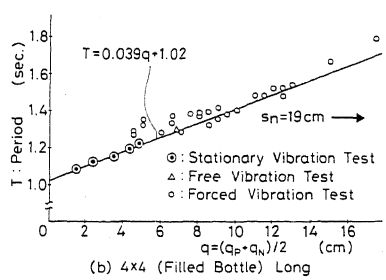

(b) 4x4 (Filled Bottle) Long

Fig 3 Relation between first mode period and top displacement amplitude

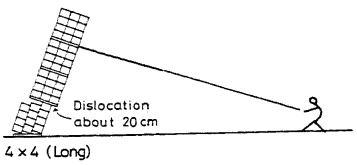

Fig 4 Observed collapse mode during the forced vibration test

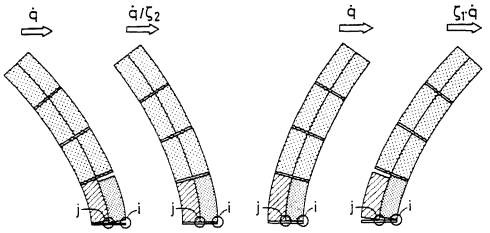

Fig 5 Conservation of angular momentum

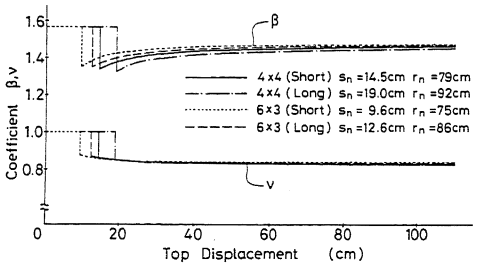

Fig 6 Participation factor β and strength factor ν

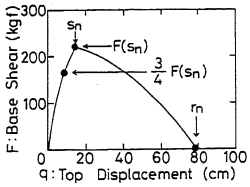

Fig 7 Calculated F-q relation of 4x4 (short)

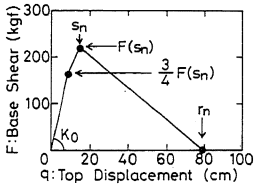

Fig 8 Trilinear F-q model for 4x4 (short)

Table 1 Data for earthquake response analysis

		Me (kg)	he* (%)	K0 (kgf/cm)	sn (cm)	F(sn) (kgf)	rn (cm)	β	ν	ζ1	ζ2
4x4	Short	1033	5.0 (0.0)	18.7	14.5	221	79	1.56(1.43)	1.0(0.832)	0.808	0.848
	Long			22.5	19.0	251	92	1.56(1.42)	1.0(0.829)	0.799	0.851
6x3	Short	610		14.5	9.6	120	75	1.56(1.42)	1.0(0.840)	0.822	0.852
	Long			14.9	12.6	135	86	1.56(1.42)	1.0(0.838)	0.816	0.854

$*he = \frac{Ce}{2\sqrt{\frac{K_0}{Me}}}$

Data in parentheses indicate values during uplifting

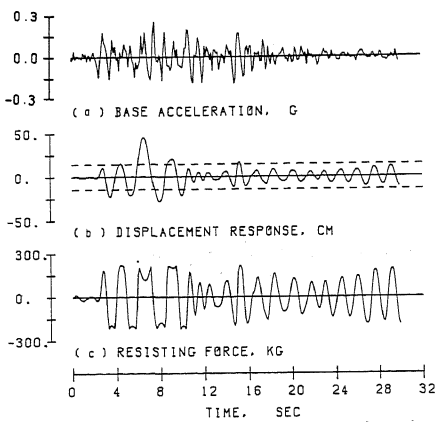

Fig 9 Response of 4x4 (short) by Miyagi earthquake

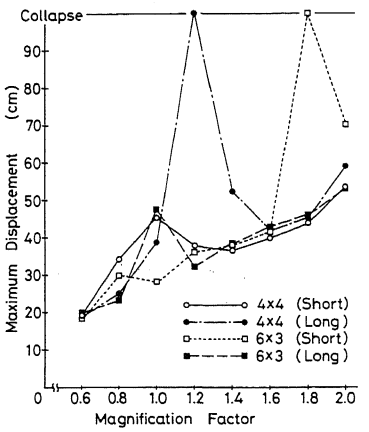

Fig 10 Response of 4 models by Miyagi earthquake